[Tanzania Journal of Engineering and Technology](https://commons.udsm.ac.tz/tjet)

Volume 44
Issue 4 *Tanzania Journal of Engineering and Technology*

Article 2

2025

# Numerical Simulation of Corner Reinforced Concrete Column-Beam Joint with Differential Concrete Grades and Steel Fibres Under Monotonic Loading

Daudi S. Augustino
*Department of Structural and Construction Engineering, University of Dar es Salaam, Dar es Salaam, Tanzania*, augustino.daudi@udsm.ac.tz

Emmanuel Safari Leo
*Department of Structural and Construction Engineering, University of Dar es Salaam, Dar es Salaam, Tanzania*, leo.emmanuel@udsm.ac.tz



## Recommended Citation

Augustino, D. S., & Leo, E. S. (2025). Numerical Simulation of Corner Reinforced Concrete Column-Beam Joint with Differential Concrete Grades and Steel Fibres Under Monotonic Loading. *Tanzania Journal of Engineering and Technology, 44*(4), 17-26. https://doi.org/10.65085/2619-8789.1043

Tanzania Journal of Engineering and Technology 2025, **44**(4):17-26
OPEN ACCESS articles distributed under Creative Commons
Attribution Licence [CC BY-ND]
Websites: https://commons.udsm.ac.tz/tjet/; https://ajol.org/tjet


ISSN 1821-536X (**print**); ISSN 2619-8789 (**electronic**)
https://doi.org/10.65085/2619-8789.1043

*Regular Research Manuscript*

# Numerical Simulation of Corner Reinforced Concrete Column-Beam Joint with Differential Concrete Grades and Steel Fibres Under Monotonic Loading

**Daudi S. Augustino† and Emmanuel S. Leo**

Department of Structural and Construction Engineering, University of Dar es Salaam, Dar es Salaam, Tanzania
†Corresponding Author: augustino.daudi@udsm.ac.tz: ORCID: 0000-0003-1843-0861

## ABSTRACT

*Structural elements are composed of joints that are essential for force transfer. In particular, for concrete structures, the column-beam joint is an integral section that requires insight due to the traditional use of different concrete grades, forming a strong-column-weak-beam (SCWB) system. A numerical model of the joint was developed in Abaqus to explore the axial load performance and damage tolerance of corner column-beam joints with different concrete grades under monotonic static loading. A concrete-damaged plasticity model (CDPM) was used to model the damage behaviour of concrete, utilising the available strain-stress models in literature and EuroCode 2. Results show that concrete column-beam joints with low grade (25 MPa) fail significantly compared to concrete cores with 30 MPa. In addition, an increase in concrete grade to 30 MPa in the joint increases the load-carrying capacity by 5.6% compared with the column joint with a concrete grade of 25 MPa. Therefore, using weak concrete joints results in axial high compressive stress exceeding the compressive strength limit, which may lead to cracks in the joint core and adjoining structural elements. It is recommended that structural engineers use the same grade for columns and beams, or use the lowest compressive strength in design, to prevent overloading the weak joint.*

ARTICLE INFO
Submitted: **Jan. 6, 2025**
Revised: **Aug. 30, 2025**
Accepted: **Oct. 3, 2025**
Published: **Dec. 2025**

**Keywords:** *Strong-column-weak-beam; Axial load performance; Monotonic loading; Concrete-damaged plasticity model; Concrete-beam Joint*

## Highlights

- Concrete joints transfer forces between members usually with different concrete grades forming a strong-column–weak-beam (SCWB) system.
- SCWB system enables beam ductility while keeping columns elastic, and it is applied even in low-seismic regions.
- Concrete grade differences cause stiffness mismatches, leading to cracks around columns and durability concerns.
- Numerical results show low-grade concrete (25 MPa) deforms excessively, while higher-grade concrete (30 MPa) reduces dilation and increases joint axial capacity.

## INTRODUCTION

### Background and motivation

The joint in structures is an integral part that transfers forces from one member to another, regardless of the material used. In particular, joints in reinforced concrete frames, such as column-to-beam joints, are critical zones that resist axial forces, shear forces, and bending moments. Therefore, these joints influence the general strength performance of framed concrete structures under monotonic loadings. The study by Allam et al. (2018) revealed that the strength performance of the exterior column-beam joint increases as the compressive strength of the entire joint increases, regardless of the boundary conditions. Compared to interior column-beam joints, the compressive strength of concrete in exterior and corner column-beam joints lacks the confinement of slabs and beams in all directions, reducing load transfer in the section (Choi et al., 2020). The concrete in confinement, such as steel tubes or columns with beams/slabs in all directions, increases resistance to compressive failure (Isleem et al., 2022, 2023). This indicates that with an increase in compressive resistance, the joint's axial capacity and moment resistance increase (BS8110-1,1997). Besides the compressive strength of concrete, other parameters, such as the cross-sections of the column and beam, their respective lengths, and the amount of reinforcement in the joint, also affect the performance of the column-beam joint. These parameters determine the joint's stiffness as a function of geometry and material. Generally, joints with lower stiffness tend to affect global stability parameters (second-order effects), such as internal forces and displacements under static loads (Patil & Manekari, 2008; SANTOS et al., 2018).

In most practices, the concrete in the column-beam joint is typically less than the concrete grade for the column. This difference in concrete grades is called strong-column-weak-beam (SCWB) and is intended to permit the formation of plastic hinges in beams before columns for structures built in earthquake zones, preventing a sudden collapse of the structure (Shamszadeh & Maleki, 2022). In seismic design, energy dissipation, stiffness degradation, and ductility are vital parameters for assessing a structure's seismic performance. The study conducted by (Gao et al. (2021) showed that an increase in axial load ratio has less influence on ductility and therefore affects the selection of SCWB. Structures' yielding mechanism and ductility depend on material strength, section size and reinforcement ratio(EN 1998-1:2004; Smarzewski, 2018). In the SCWB criteria, the less-strength beams are ductile, so the formation of plastic hinges in columns is delayed due to the lower stiffness ratio of the joint(Su et al., 2020). Despite this advantage, a less concrete joint can affect the overall deformation of the structural system and impede the load transfer. In this case, composite concrete with steel fibres is a paramount consideration to avoid a compromise in compressive strength while maintaining the ductility of the column-beam joint. Steel fibres increase the ductility and stiffness of high-strength concrete and promote the application of steel fibre-reinforced sections in both monotonic and dynamic load configurations(Augustino et al., 2023; Augustino, Kabubo, et al., 2022; Augustino, Onchiri, et al., 2022).

In areas with no earthquake history, low concrete strength in column-beam joints is less significant in static load-carrying capacity. Concrete with low glades shrinks more than concrete with high-strength (Augustino et al., 2023). Concrete shrinkage reduces sections, resulting in weak stiffness of the beam and, therefore, shrinkage affects weak column-beam joints at high axial load (Lampropoulos & Dritsos, 2011). For this case, SCWB criteria may result in the shrinkage of the column-beam joint, affecting the overall transfer of internal forces through the joint. A numerical model by Yu et al. (2013) confirmed that using sandwich layers of concrete in the column-beam joint produces a joint with excessive compressive stress. In addition, the column positions in structural concrete frames influence joint performance. For instance, the corner and exterior columns suffer a slight rotation of the beams compared to the inner columns(Alva & El Debs, 2013). This rotation can significantly affect SCWB joints, leading to cracks that compromise the joint core's durability.

## Research Significance

Despite the strong-column weak-beam/slab approach aiming to permit ductility in beams, allowing plastic deformation while maintaining the elastic regime of columns in a seismic environment, this practice has been adopted in several areas, even in regions with low seismicity. This has resulted in several cracks around the columns for high-rise buildings propagating towards slabs and beams due to differential material stiffnesses and stress transfer. Cracks around the column may impede the durability of the reinforced concrete section due to the ingress of corrosion agents. This study will numerically explore the axial load performance and damage capability of corner column-beam joints with different concrete grades under monotonic static loading. In addition, the study will deploy steel fibre mesh to limit local deformations at the column-beam interface. Steel fibres can increase the stiffness of the resulting concrete and reduce the risk of serviceability failure in concrete sections. The results of this study will be of significant importance to structural design engineers in areas with a design ground acceleration of seismic excitation less than 0.39 m/s$^2$ (EN 1998-1: Eurocode 8: 2004).

# METHODS AND MATERIALS

## Numerical Modelling

### *Geometry of Structural Elements*

The concrete column-beam joint was modelled in Abaqus/CAE (Python scripting). The beam in the column-beam joint had a cross-section size of 250 x 250 mm. Since the primary focus is shear forces in the joint, the overall beam length was set to 1000 mm. The columns, both above and below the joint, had a cross-section of 250 x 250 mm and a length of 1000 mm each. The steel reinforcements for the column and beam were four, with 16- and 12-mm diameters, respectively, with stirrup steel reinforcements of 8 mm in diameter. A 250 x 250 mm steel plate with a thickness of 20 mm was used to limit excessive stresses at the point where the load was applied.

### *Material Models*

Compared to other materials, concrete is ductile under compression. The concrete for the columns in this study had a compressive cube strength of 30 MPa, while the beams had either 25 or 30 MPa. The column-beam joint was set for both grades, i.e., 25 and 30 MPa, implying that the concrete has a hybrid layer of 25 MPa and 30 MPa and with only 30 MPa. Therefore, the column-beam joint with concrete grade 25 MPa was named C30_B25 while that with 30 MPa was named C30_B30. Since Eurocode was used to estimate some parameters, an equivalent cylinder compressive strength was used. Based on Eurocode 2, the yield strength was 40% of the compressive strength. In this region, the elastic modulus as a measure of concrete stiffness was deduced using Equation (1), as in Eurocode 2. To estimate the concrete strain corresponding to the maximum compressive strength of concrete, Equation (2) was used. The peak tensile strength of concrete was deduced using its compressive strength in Equation (3). Stress-strain curves of concrete in compression and tension were established using Equations (4) and (5), respectively, as shown in Figure 1. The constant $\kappa$ and $\eta$ were established using Equations (6) and (7), respectively.

In Equations, $E_c$ in an elastic Young's Modulus in a compression load setup, $f_{cu}$ is the compressive strength of concrete, $\varepsilon_{cu}$ is compressive strain corresponding to compressive strength, $\sigma_{tu}$is tensile strength of concrete, $\sigma_c$ is compressive stress, $\kappa$ is the stress coefficient, $\eta$ is the strain coefficient, $\sigma_t$ tensile stress, $\varepsilon_t$ is tensile strain, $\varepsilon_{tu}$ is tensile strain corresponding to tensile strength, $\varepsilon_c$ is compressive strain.

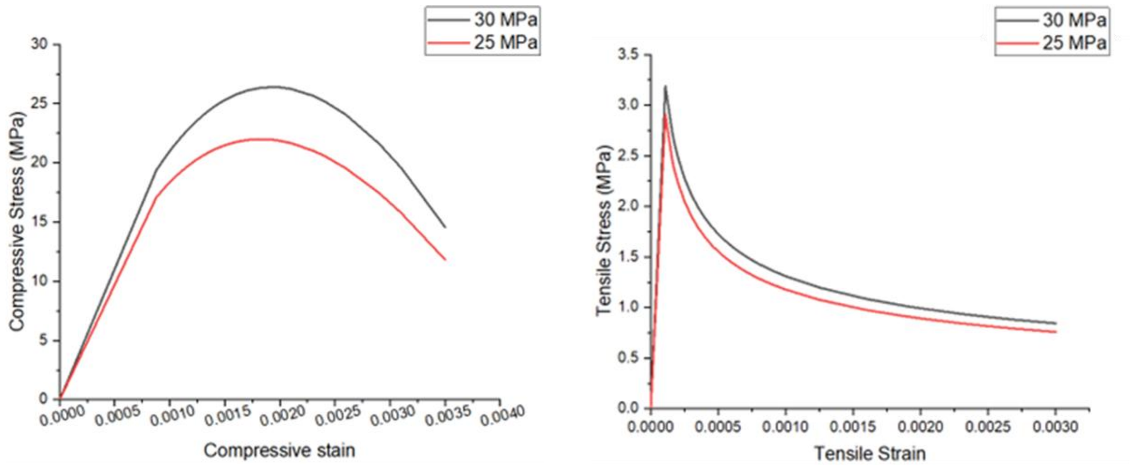


**Figure 1: Stress-strain Curves (a) Compressive behaviour and (b) Tensile behaviour.**

$$E_c = 22\left(\frac{f_{cu}}{10}\right)^{0.3} \quad (1)$$

$$\varepsilon_{cu} = \frac{0.7(f_{cu})^{031}}{1000} \quad (2)$$

$$\sigma_{tu} = 0.62\sqrt{f_{cu}} \quad (3)$$

$$\sigma_c = \frac{f_{cu}(\kappa\eta - \eta^2)}{1 + (\kappa - 2)\eta} \quad (4)$$

$$\sigma_t = \begin{cases} E_c\varepsilon_t \quad , & \varepsilon_t \leq \varepsilon_{tu} \\ \sigma_{tu}\left(\frac{\varepsilon_{tu}}{\varepsilon_t}\right)^{0.4}, & \varepsilon_t > \varepsilon_{tu} \end{cases} \quad (5)$$

$$\kappa = 1.05\frac{E_c\varepsilon_{cu}}{f_{cu}} \quad (6)$$

$$\eta = \frac{\varepsilon_c}{\varepsilon_{cu}} \quad (7)$$

A concrete-damaged plasticity model (CDPM) was used to model concrete in Abaqus. The default plasticity properties for concrete were used as in Table 1. To define concrete's compressive and tensile behaviour to failure, stress was taken from yield, damage parameters, and crushing/cracking strains were used, as shown in Table 2. All Equations used to develop the stress-strain curve were from Eurocode 2, except for the tensile stress-strain curve model, which was deduced using literature(Rai, 2021). This model is used when there is no continuous record of strain and stress in the test setup. The crushing and cracking strains were developed using Equations (8) and (9), respectively (Augustino, 2024; Hafezolghorani et al., 2017). For the steel reinforcement, Young's modulus, tensile strength, and Poisson's ratio of 210000 MPa, 500 MPa, and 0.3 were used in modelling, respectively. Equation (10) was used to quantify the extent of concrete damage in compression and tension. The damage is zero at peak stress and 1 as the tension or compression stress decreases from peak to zero in the descending part of the stress-strain curves.

**Table 1: Plasticity parameters**

| Angle of dilation | Eccentricity | fbo/fco | K | Viscosity |
|---|---|---|---|---|
| 30° | 0.1 | 1.16 | 0.67 | 0.00001 |

**Table 2: Inelastic strains and damage parameters of concrete**

| Concrete grade 30 | | | | Concrete grade 25 | | | |
|---|---|---|---|---|---|---|---|
| **Crushing strain** | **Damage C** | **Cracking strain** | **Damage T** | **Crushing strain** | **Damage C** | **Cracking strain** | **Damage T** |
| 0 | 0 | 0 | 0 | 0 | 0 | 0 | 0 |
| 0.00031 | 0 | 0.00006 | 0.1448 | 0.00036 | 0 | 0.000073 | 0.1571 |
| 0.00034 | 0 | 0.00007 | 0.1652 | 0.00040 | 0 | 0.000082 | 0.1773 |
| 0.00039 | 0 | 0.00008 | 0.1841 | 0.00046 | 0 | 0.000092 | 0.1959 |
| 0.00044 | 0 | 0.00010 | 0.2178 | 0.00050 | 0 | 0.00011 | 0.2291 |
| 0.00047 | 0 | 0.00015 | 0.2846 | 0.00053 | 0 | 0.00016 | 0.2949 |
| 0.00050 | 0 | 0.00020 | 0.3349 | 0.00056 | 0 | 0.00021 | 0.3445 |
| 0.00053 | 0 | 0.00025 | 0.3747 | 0.00059 | 0 | 0.00026 | 0.3837 |
| 0.00055 | 0 | 0.00030 | 0.4072 | 0.00061 | 0 | 0.00031 | 0.4158 |
| 0.00057 | 0 | 0.00035 | 0.4345 | 0.00063 | 0 | 0.00036 | 0.4426 |
| 0.00059 | 0 | 0.00040 | 0.4578 | 0.00065 | 0 | 0.00041 | 0.4656 |
| 0.00061 | 0 | 0.00045 | 0.4781 | 0.00067 | 0 | 0.00046 | 0.4856 |
| 0.00063 | 0 | 0.00050 | 0.4959 | 0.00069 | 0 | 0.00051 | 0.5032 |
| 0.00065 | 0 | 0.00055 | 0.5118 | 0.00071 | 0 | 0.00056 | 0.5189 |
| 0.00067 | 0 | 0.00060 | 0.5261 | 0.00073 | 0 | 0.00061 | 0.5329 |
| 0.00069 | 0 | 0.00065 | 0.5390 | 0.00075 | 0 | 0.00066 | 0.5456 |
| 0.00071 | 0 | 0.00070 | 0.5507 | 0.00077 | 0 | 0.00071 | 0.5572 |
| 0.00073 | 0 | 0.00080 | 0.5714 | 0.00079 | 0 | 0.00081 | 0.5776 |
| 0.00075 | 0 | 0.00090 | 0.5891 | 0.00081 | 0 | 0.00091 | 0.5950 |
| 0.00077 | 0 | 0.00115 | 0.6242 | 0.00083 | 0 | 0.00116 | 0.6296 |
| 0.00087 | 0 | 0.00150 | 0.6595 | 0.00093 | 0 | 0.00151 | 0.6644 |
| 0.00097 | 0 | 0.00180 | 0.6821 | 0.00103 | 0 | 0.00181 | 0.6867 |
| 0.00107 | 0 | 0.00190 | 0.6886 | 0.00113 | 0 | 0.00191 | 0.6931 |
| 0.00120 | 0 | 0.00220 | 0.7055 | 0.00126 | 0.0022 | 0.00221 | 0.7098 |
| 0.00127 | 0.001 | 0.00240 | 0.7152 | 0.00133 | 0.0062 | 0.00241 | 0.7193 |
| 0.00137 | 0.006 | 0.00260 | 0.7238 | 0.00143 | 0.0152 | 0.00261 | 0.7278 |
| 0.00157 | 0.0278 | 0.00290 | 0.7352 | 0.00163 | 0.0440 | 0.00291 | 0.7390 |
| 0.00167 | 0.0445 | | | 0.00173 | 0.0635 | | |
| 0.00187 | 0.0888 | | | 0.00193 | 0.1121 | | |
| 0.00217 | 0.1808 | | | 0.00223 | 0.2066 | | |
| 0.00237 | 0.2582 | | | 0.00243 | 0.2829 | | |
| 0.00277 | 0.4481 | | | 0.00283 | 0.4629 | | |

$$\varepsilon_{crushing} = \varepsilon_c - \frac{\sigma_{cy}}{E_C} \quad (8)$$

$$\varepsilon_{cracking} = \varepsilon_t - \frac{\sigma_{ty}}{E_C} \quad (9)$$

$$d = 1 - \frac{\sigma}{\sigma_u} \quad (10)$$

whereas; $\varepsilon_{crushing}$ is the crushing strains, $\sigma_{cy}$ is yield compressive stress, $\varepsilon_{cracking}$ is the cracking strains, $\sigma_{ty}$ is cracking strains, $d$ is the damage parameter in tension or compression, $\sigma$ is the tensile or compressive stresses in a descending order from peak stress, $\sigma_u$ is the tensile or compressive stress/strength of concrete. Other variables are as previously defined.

*Loading, Interaction and Boundary Conditions*

The limit for deflection in a beam was set to be span/250 (EN 1992-1-1:2004). Therefore, the vertical prescribed deflection of 4 mm was applied parametrically at the end of the beam to assess deformation in the structural joint. The same value (deflection of 4 mm) was used on top of the column as the axial displacement of a column, which is less than the allowable settlement of 25 mm prescribed in (EN 1997-1: 2004). Although concrete in the joint is cast in three phases: column, then the beam, and finally the top column, the column-beam interface is usually strong enough to prevent slip. Therefore, the tie constraint was used to simulate the friction resistance of the column-beam interface. Since the regular column has a total length of more than 3 m, the selected segment of 1000 mm below the joint implies that the end of the segment has a moment regardless of the boundary condition of the ideal full column length. In this case, the bottom end of the bottom column in the model was set to allow neither rotation nor displacement, as shown in Figure 2(a). The bottom part of the beam at the joint was kinematically coupled, as in the scripts of Figure 2(b), to the reference point where stress and reactions were probed. Steel reinforcements, steel fibres, and concrete were constrained using a truss-in-solid embedded constraint in Abaqus to limit only translational displacements. The rotational degree of freedom was set free to allow the rotation of the rebar and fibres in case of excessive joint deformation.

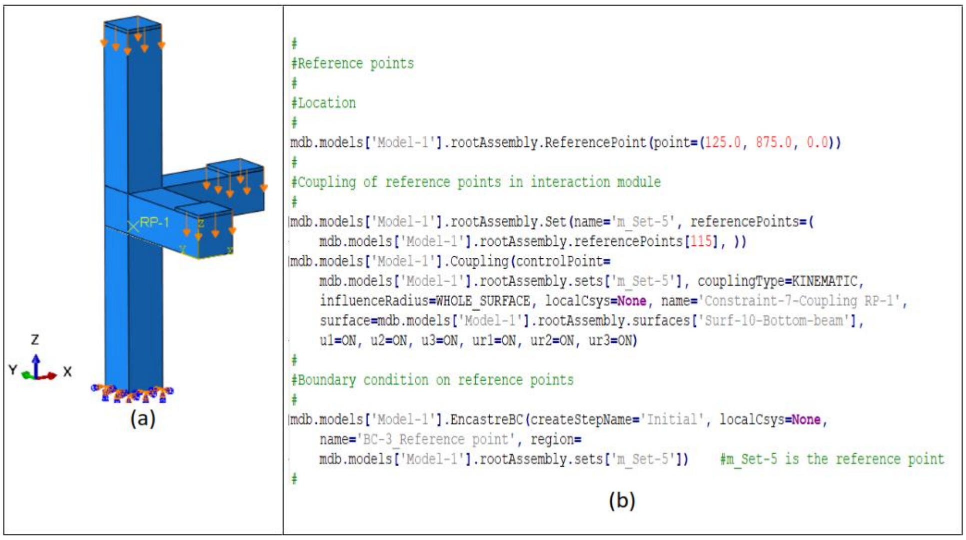


**Figure 2: Loading and boundary conditions and (b) Parametric Python scripts used in the coupling of the beam surface and the reference point**

*Finite element type and analysis*

Partition techniques were used to obtain a structured mesh. The mesh size was set to 30 mm. The concrete beam and column mesh were assigned C3D8, an 8-node linear hexahedron finite element with reduced integration and hourglass control. On the other hand, steel reinforcement and fibres were assigned the T2D3 element, a 2-node linear 3-D truss element. The analysis in Abaqus/Standard is an implicit solver which uses Newton's method to solve nonlinear problems. This solver does not have automatic stability as an explicit solver (Abaqus/Explicit).

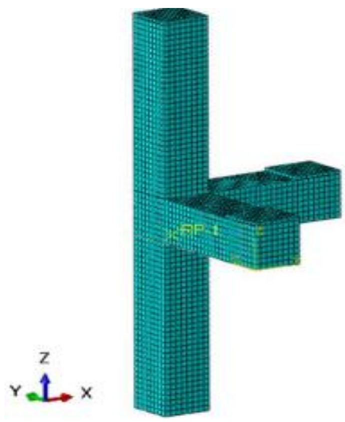


**Figure 3: Meshing type.**

It typically seeks stability/equilibrium through iteration in step increments, checking the difference between the externally applied load and the internal reactions/forces obtained. This difference must approach zero before moving to another step increment. To enhance the model's stability and convergence, the number of increments was increased parametrically in the step module.

## RESULTS AND DISCUSSION

### Failure modes

The results in Figures 4, 5, and 6 are plots of the stress distribution in steel reinforcement, and of concrete damage in compression and in tension, respectively. Results in Figure 4 show that a column-beam joint with fibre mesh increases stiffness, leading to higher joint stress and increased stress in the steel reinforcements. This agrees with Augustino, Kabubo, et al. (2022) on the effect of steel fibres in taking up tensile stress. Despite the same failure modes in Figure 4 (b), fibres seem to take the stress, which reduces stresses in stirrups above the column and on the top reinforcements in beams compared to joints without steel fibres

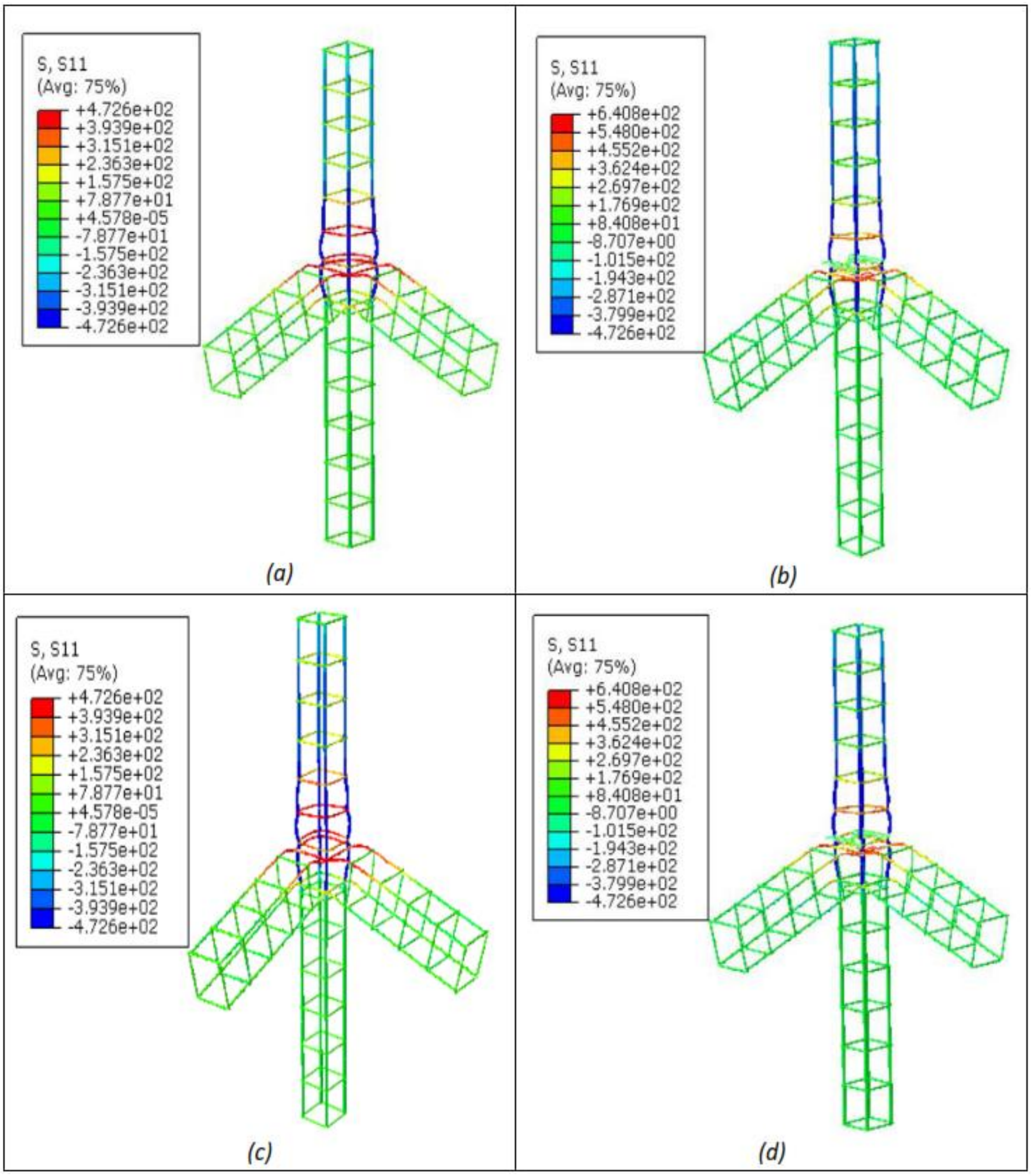


**Figure 4: Stress distribution in steel reinforcements; (a) C30_B25 without fibres, (b) C30_B25 with fibres, (c) C30_B30 without fibres and (d) C30_B30 with fibres.**

In Figure 4 (a) and (c), concrete joints without fibres, the stirrups were highly stressed, justifying the demand for less spacing of stirrup steel reinforcements just above the joint. Since the damage model is for concrete, the fibre mesh does not affect the concrete's failure. For a joint with a lower concrete grade, that is, a beam with a concrete grade of 25 MPa, the whole joint fails under excessive compression, compared to a beam with 30 MPa that fails partially, with the primary failure being at the bottom part of the top column, as in Figures 5 (c) and (d). This failure of the joint with 25 MPa, Figures 5(a) and (b), aligns with Isleem et al. (2023), which indicates that concrete with lower strength dilates more than concrete with higher strength. Therefore, the joint with a concrete beam at 30 MPa showed no concrete dilation, i.e., no volumetric failure. This trend could be due to increased joint stiffness as concrete's compressive strength increases. The same failure trend was observed in tension as in Figure 6. These failure modes of concrete can detrimentally affect the service life of column-beam concrete joints by forming cracks around them, accelerating the ingress of corrosion agents and thereby affecting the durability of the joint in service of the structure.

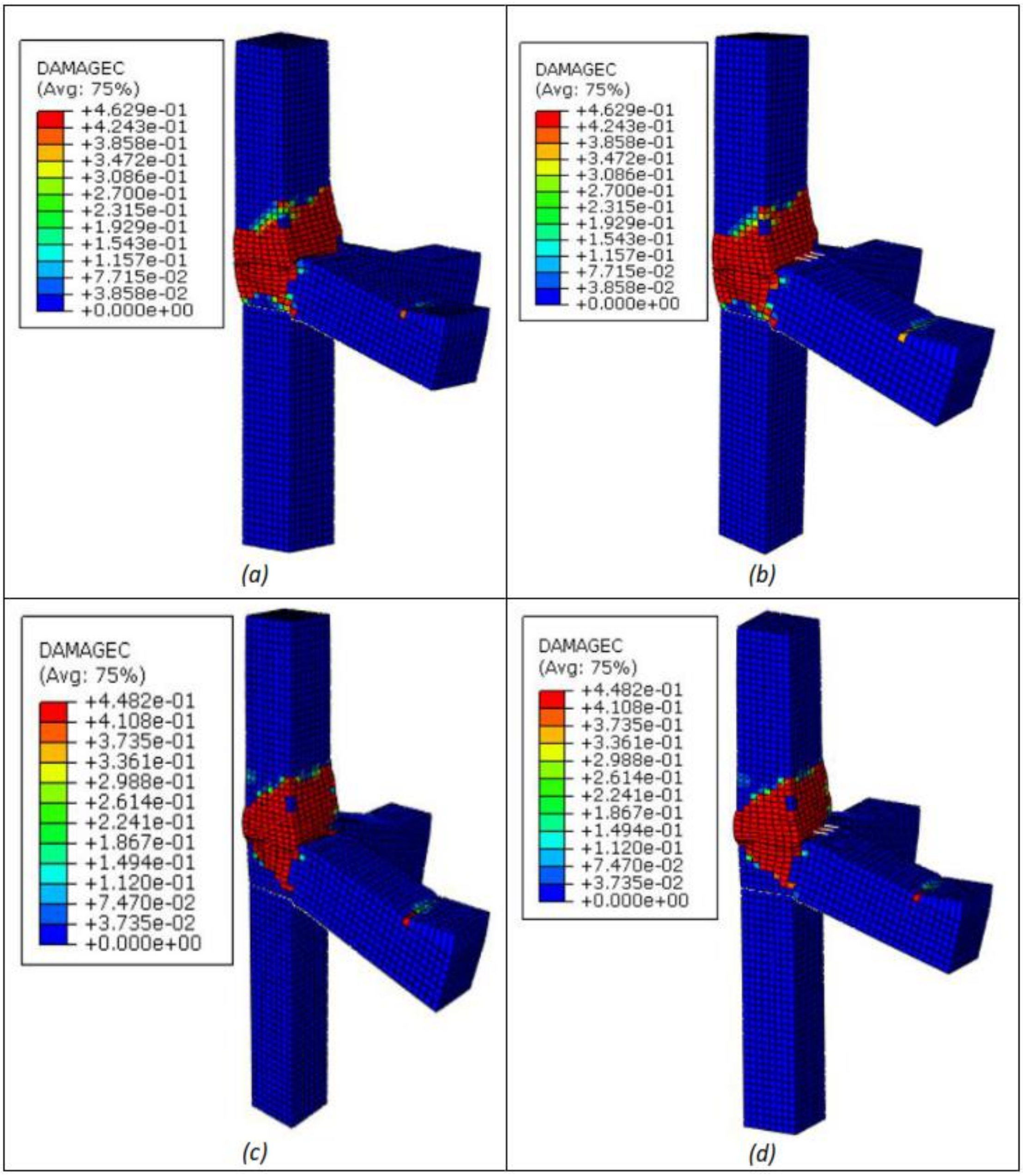


**Figure 5: Concrete damage in compression; (a) C30_B25 without fibres, (b) C30_B25 with fibres (c) C30_B30 without fibres and (d) C30_B30 with fibres.**

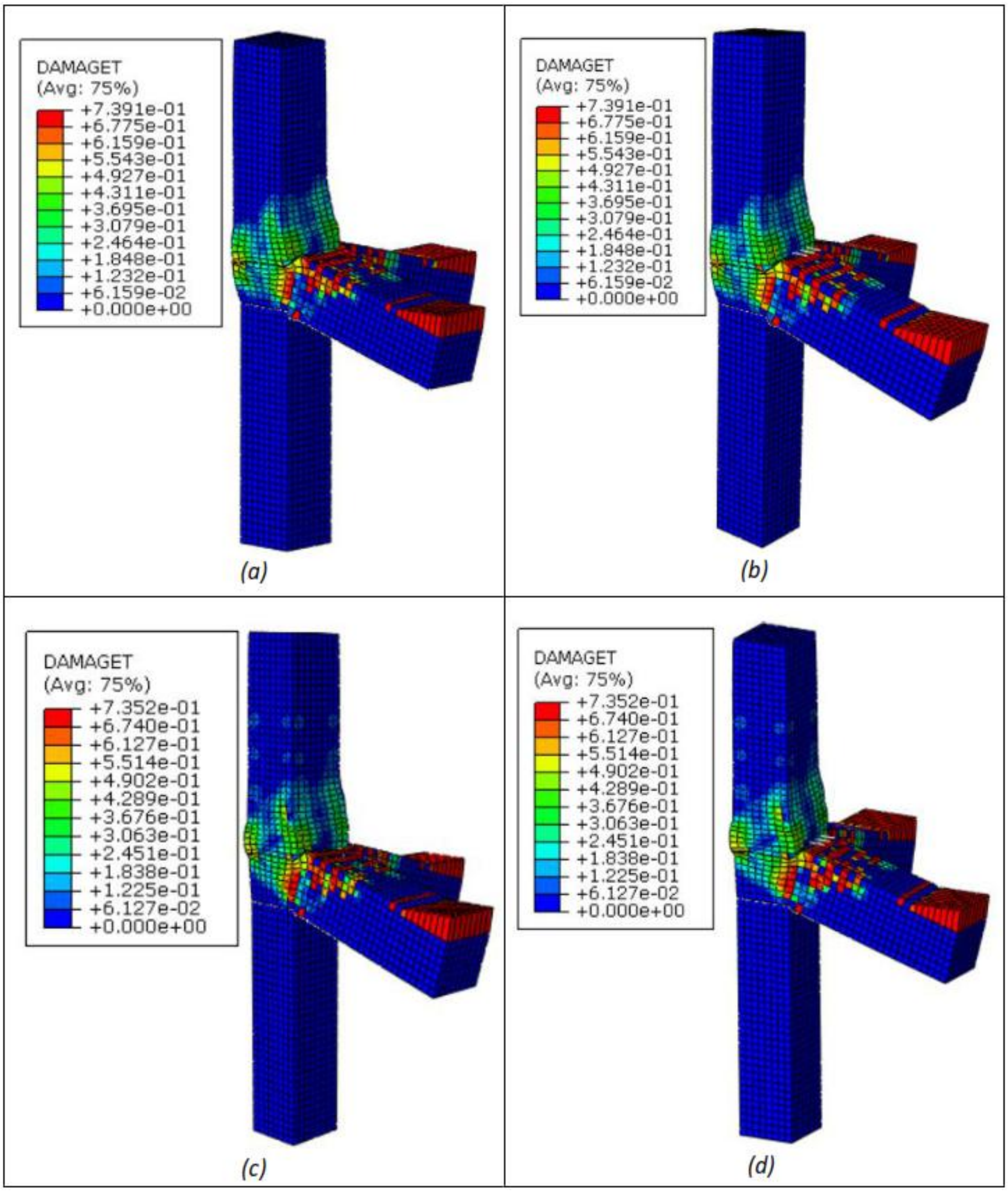


**Figure 6: Concrete damage in tension; (a) C30_B25 without fibres, (b) C30_B25 with fibres (c) C30_B30 without fibres and (d) C30_B30 with fibres.**

## Load Capacity of the Column-Beam Joint

Figure 7 presents the axial load capacity for different column-beam joints with different concrete grades and fibres. The results show that fibres have an insignificant contribution to axial load capacity. For instance, in a column joint with concrete grade 25 MPa, adding fibre increases the load-carrying capacity by only 0.003%. This slight increase reflects the tensile-dominant load-carrying behaviour of steel fibres compared to compression. The column joint is under compression loading; therefore, fibre mesh could improve serviceability cracking and ductility rather than increasing joint stiffness. However, adding fibres to the concrete matrix rather than a fibre mesh could significantly increase the load capacity (Liu et al., 2024). Furthermore, with the joint's concrete grade increased to 30 MPa, the load-carrying capacity increased by 5.6% compared with the column joint with a concrete grade of 25 MPa. These results concur with those of Allam et al. (2018), who found that an increase in concrete compressive strength is associated with an increase in elastic modulus, implying less deformation and therefore a higher load being carried. For a weak concrete joint, the resulting axial compressive stress in the joint core could exceed the joint's compressive strength, leading to cracks in the joint core and adjoining structural elements. These excess stresses in structural columns expose users to risk, as columns are a crucial part of the structural integrity of the frames.

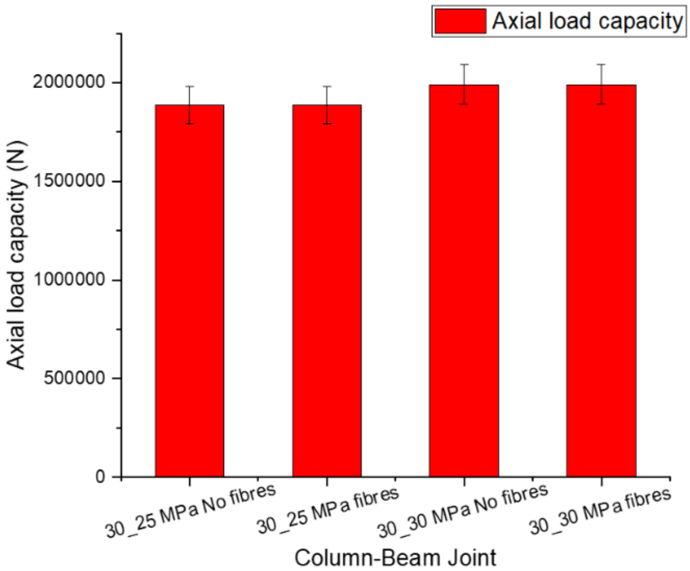


**Figure 7: Axial load capacity for different column-beam joints with different concrete grades and fibres.**

## CONCLUSION AND RECOMMENDATIONS

The study aimed to explore numerically the axial load performance and damage capability of corner column-beam joints with different concrete grades under monotonic static loading. The following are the conclusions and recommendations.

i) The core concrete in the column-beam joint with a low grade, 25 MPa, deformed excessively compared to the concrete grade 30 MPa. This deformation of concrete grade 25 MPa results from the compressive capacity of the section being exceeded.

ii) Using fibre mesh in the column-beam joint can significantly reduce the stress concentration in the steel reinforcement. However, it has an insignificant effect on the overall axial compression capacity of the joint.

iii) The high strength of both columns and beams increases the axial load capacity of the joint and limits the dilation of the concrete core in the joint.

Due to the significant dilation effect and low axial capacity of concrete with low grade in the column-beam joint, structural engineers, when using available design tools and software, should consider, upon the necessity of having a different concrete grade arise, a low concrete grade to be used in the design of structural frames. It could be expensive for high-rise buildings that require strong columns if all horizontal members, such as beams and slabs, are of the same grade. Instead, it is recommended during the beam and slab construction to have a special concrete grade in the joint, similar to that of the column. Although this may seem tedious, it can save the costs of having a strong concrete grade throughout the building. Additionally, it reduces excessive joint stress when using low concrete grades, thereby enhancing the durable performance of the column-beam joint.

## REFERENCES


Allam, S. M., Elbakry, H. M. F., & Arab, I. S. E. (2018). Exterior reinforced concrete beam column joint subjected to monotonic loading. *Alexandria Engineering Journal*, **57**(4), 4133–4144. doi: 10.1016/j.aej.2018.10.015

Alva, G. M. S., & El Debs, A. L. H. de C. (2013). Moment-rotation relationship of RC beam-column connections: Experimental tests and analytical model. *Engineering Structures*, **56,** 1427–1438. doi: 10.1016/j.engstruct.2013.07.016

Augustino, D. S. (2024). Shear Performance of Deep Concrete Beams with Openings Using Waste Tyre Steel Fibres: FEM and ANN Analysis. *Civil Engineering Journal*, **10**(8), 2422–2449. d doi: 10.28991/CEJ-2024-010-08-02

Augustino, D. S., Kabubo, C., Kanali, C., & Onchiri, R. O. (2022). The orientation effect of opening and internal strengthening on shear performance of deep concrete beam using recycled tyre steel fibres. *Results in Engineering*, **15**, 100561. doi: 10.1016/j.rineng.2022.100561

Augustino, D. S., Kanali, C., Onchiri, R. O., & Kabubo, C. (2023). Simplified shear equation of deep concrete beam considering orientation effect of opening and mechanical properties of fibre-concrete interface. *Heliyon*, **9**(3), e14441. doi: 10.1016/J.HELIYON.2023.E14441

Augustino, D. S., Onchiri, R. O., Kabubo, C., & Kanali, C. (2022). Mechanical and Durability

Performance of High-Strength Concrete with Waste Tyre Steel Fibres. *Advances in Civil Engineering*, *2022*.

*BS 8110-1: Structural use of concrete - design & construction*. (1997)

Choi, S. H., Hwang, J. H., Han, S. J., Cho, H. C., Kim, J. H., & Kim, K. S. (2020). Simplified Effective Compressive Strengths of Columns with Intervening Floor Slabs. *International Journal of Concrete Structures and Materials*, **14**(1), doi: 10.1186/s40069-020-00419-8

*EN 1992-1-1: Eurocode 2: Design of concrete structures - Part 1-1: General rules and rules for buildings*.(2004)

*EN 1997-1: Eurocode 7: Geotechnical design - Part 1: General rules*. (2004).

*EN 1998-1: Eurocode 8: Design of structures for earthquake resistance – Part 1: General rules, seismic actions and rules for buildings*. (2004).

Gao, F., Tang, Z., Mei, S., Hu, B., Huang, S., & Chen, J. (2021). Seismic behavior of exteriorbeam–column joints withhigh-performance steel rebar: Experimental and numerical investigations. *Advances in Structural Engineering*, **24**(1): 90–106. doi: 10.1177/1369433220942870

Hafezolghorani, M., Hejazi, F., Vaghei, R., Jaafar, M. S. Bin, & Karimzade, K. (2017). Simplified damage plasticity model for concrete. *Structural Engineering International*, **27**(1), 68–78. doi: 10.2749/101686616X1081

Isleem, H. F., Augustino, D. S., Qaidi, S., Muayad, M., & Sabri, S. (2023). *Finite element , analytical , arti fi cial neural network models for carbon fi bre reinforced polymer con fi ned concrete fi lled steel columns with elliptical cross sections*. *January*, 1–18. doi: 10.3389/fmats.2022.1115394

Isleem, H. F., Peng, F., & Tayeh, B. A. (2022). Confinement model for LRS FRP-confined concrete using conventional regression and artificial neural network techniques. *Composite Structures*, **279**, 114779. doi: 10.1016/J.COMPSTRUCT.2021.114779

Lampropoulos, A. P., & Dritsos, S. E. (2011). Concrete shrinkage effect on the behavior of RC columns under monotonic and cyclic loading. *Construction and Building Materials*, **25**(4), 1596–1602. doi: 10.1016/j.conbuildmat.2010.10.001

Liu, X., Pan, M., Li, W., Jing, C., Chang, W., & Zhang, H. (2024). Experimental Study and Bearing Capacity Calculation of Compression-Reinforced Concrete Columns Strengthened with Ultra-High-Performance Concrete. *Applied Sciences (Switzerland)*, **14**(5), doi: 10.3390/app14051911

Patil, S. S., & Manekari, S. S. (2008). Analysis of Reinforced Beam-Column Joint Subjected to Monotonic Loading. In *Certified International Journal of Engineering and Innovative Technology (IJEIT)* (Vol. 9001, Issue 10).

Rai, P. (2021). Non-Linear Finite Element Analysis of RC Deep Beam Using CDP Model. *Advances in Technology Innovation*, **6**(1), 01–10. doi: 10.46604/aiti.2021.5407

SANTOS, J. B., SILVA, T. J. DA, & ALVA, G. M. S. (2018). Influence of the stiffness of beam-column connections on the structural analysis of reinforced concrete buildings. *Revista IBRACON de Estruturas e Materiais*, **11**(4), 834–855. doi: 10.1590/s1983-41952018000400010

Shamszadeh, M. M., & Maleki, S. (2022). Evaluation of strong column-weak beam criterion in spliced columns of steel moment frames. *Results in Engineering*, **14**, doi: 10.1016/j.rineng.2022.100453

Smarzewski, P. (2018). Analysis of failure mechanics in hybrid fibre-reinforced high-performance concrete deep beams with and without openings. *Materials*, **12**(1), doi: 10.3390/ma12010101

Su, J., Liu, B., Xing, G., Ma, Y., & Huang, J. (2020). Influence of Beam-to-Column Linear Stiffness Ratio on Failure Mechanism of Reinforced Concrete Moment-Resisting Frame Structures. *Advances in Civil Engineering*, *2020*. doi: 10.1155/2020/9216798

Yu, X., Wu, N., Yang, Z., & Xu, K. (2013). Analysis of the impact of concrete compressive strength reduction in joint core area on super high-rise structures. *Applied Mechanics and Materials*, **438–439**, 690–695. doi: 10.4028/www.scientific.net/AMM.438-439.690